23rd ABCM International Congress of Mechanical Engineering
December 6-11, 2015, Rio de Janeiro, RJ, Brazil

IMPEDANCE CONTROLLED BIOMECHATRONIC EXOSKELETON WITH A SHAPE MEMORY ALLOY ACTUATOR: AN EXPERIMENTAL EVALUATION

André A. M. Araujo
Eduardo A. Tannuri
Arturo Forner-Cordero
Department of Mechatronics Engineering, Escola Politécnica, University of São Paulo,
Av. Prof. Mello Moraes, 2231, CEP 05508-970, São Paulo, Brazil
andremdaraujo@gmail.com, eduat@usp.br, aforner@usp.br

Abstract. *This work presents the experimental results of an impedance control algorithm developed and tested with the aid of a reduced scale biomechatronic exoskeleton powered by a shape memory alloy (SMA) actuator. The experimental apparatus is described, including its mechanical design, sensors used, electric driver design and system control. The test procedure is then explained, followed by the results of experimental tests on the prototype. Then, results are discussed and further improvements are suggested.*

Keywords: *Robotics, Exoskeleton, Orthose, Impedance control, Shape memory alloys*

1. INTRODUCTION

Biomechatronic exoskeletons have earned a respectful position in the current scenario of robotics engineering. Such statement can be confirmed by the extensive research on the subject (Araujo et al., 2012; Aguirre-Ollinger et al. 2007; Aral et al., 2007; Crowell III et al., 2002; Cyberdyne, 2012; Miranda et al., 2012), even including implementations in commercial phase, such as the lower limb exoskeleton Ekso (Ekso Bionics, 2014) and the POWERLOADER Light (Activelink Co., Ltd., 2014). These devices, which could also be described as robotic orthoses, are being studied for rehabilitation and strength or speed augmentation. Since they are used cooperatively with humans, their control needs to be safe and precise.

Impedance control is very useful when two or more dynamical systems interact. Therefore, it is commonly used in exoskeletons, given that controlling position or force separately might lead to inadequate or even unsafe situations, while the relationship between these quantities is the important factor to be controlled (Kim et al., 2007).

Aiming to construct lighter and more versatile exoskeletons, the search for novel components is a must (Dollar, Herr, 2008). This is not only related to the mechanical structure but also to the actuators (Raparelli, 2002). A possible alternative to the actuators commonly employed (electric motors, pneumatic and hydraulic systems) would be the use of actuators based on shape memory alloys (SMA) (De Laurentis et al., 2002). These alloys belong to the so called “intelligent materials” and present an interesting property called “shape memory effect”. This property allows them to recover a previously defined shape by the controlled use of heat (Romano, Tannuri, 2009b). Despite their control complexity, these alloys are being studied in several robotic applications, thanks to its versatility and capacity of miniaturization (Lu et al., 1997).

Taking this into account, this paper extends the work introduced previously by the authors (Araujo et al., 2012), further investigating the feasibility of using SMA actuators in exoskeletons for humans. In particular, a reduced scale, hip joint flexo-extension exoskeleton prototype is evaluated experimentally.

2. EXPERIMENTAL APPARATUS

2.1 Mechanical Design

The mechanical prototype consists of a pendulum, attached to an axle supported by two ball bearings, while the axle is connected directly to the SMA actuator. The pendulum is comprised of a bar, linked to the axle through a load cell that measures the interaction force between the user and the exoskeleton. The axle has bolts that allow the attachment of up to 4 SMA wires, although only one was used during this work. On the other side of the prototype (left side on Fig. 1), there are also bolts to fix the SMA wires. This system would also permit the use of another load cell to measure the traction force exerted by the actuator, but it was not used. As for measuring the angle, a potentiometer was installed, with its axle fixed to the pendulum axle and its base fixed to the prototype base. Considering the hip joint and flexo-extension motion, the system was designed with parameters (inertia, damping and stiffness) proportional to a human leg. The pendulum and the wire measure about 300 mm long, each. Fig. 1 shows a 3D drawing of the prototype in the design phase, with its parts described, while its mathematical model is depicted in Fig. 2.

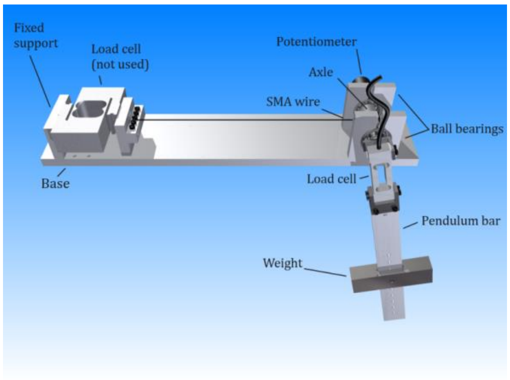

Figure 1 – 3D drawing of the prototype, with its parts described.

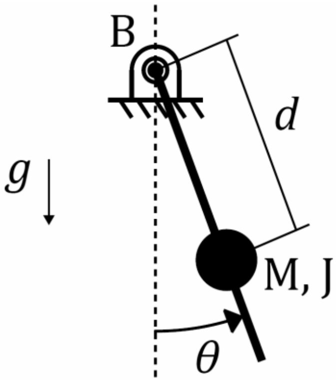

Figure 2 – Mathematical model of the prototype.

2.2 Sensors

Angular position was measured by a potentiometer with range of 300° and electrical resistance of 10 kΩ, powered by a voltage of 5V. Its signal was then routed to an analog input port of an ADC/DAC interface, to be used by the control algorithm to determine the pendulum angle. The calibration of the potentiometer was done by positioning the pendulum in the vertical (0°) and horizontal (90°) position; since the potentiometer has linear taper, two points were sufficient to derive a formula to convert the output voltage to angle.

Torque was measured by the use of a PW4MC3/300G-1 load cell (made by HBM), capable of measuring forces up to 3.0 N. Similarly to the calibration procedure of the potentiometer, the pendulum was held by the user in the vertical and horizontal positions. The load cell also has linear output with respect to the force input; therefore, these two points of calibration, together with the mass of the bar (0.120kg) and the distance between the interaction point and the rotation axis, lead to a formula to convert the load cell output voltage to torque.

2.3 Electrical driver

The contraction of the SMA occurs due to the passage of electric current through the wire, thanks to the Joule effect. Thus, the SMA driver circuit is a voltage-controlled current source with an input to output relationship of 1 A/V. One advantage of using a current source is that the output does not depend on the actuator electric resistance; therefore, many setups are possible with the same circuit.

2.4 System control

The prototype was controlled by a program developed on MATLAB R2010b, using Simulink. The interface between the program and the prototype was done by a NI USB-6008 analog-to-digital and digital-to-analog converter (ADC/DAC) made by National Instruments. During this work, an analog output generated the electrical voltage used to control the actuator driver, thus controlling the current flow through the SMA wire. Three analog inputs were used to receive: the voltage from the potentiometer, the load cell output and the voltage generated across a 1 Ω shunt resistor, which transduced the current flow through the actuator.

In order to achieve real-time processing in MATLAB to control the exoskeleton, a library called RT Blockset, developed by Daga (Daga, 2012), was used. This set of programs allow Simulink models to be executed with controlled time between steps, therefore leading to an execution that is executed approximately in real-time. The system achieved a stable sampling rate of 80 Hz which was sufficient for this application. Despite of the fact that the Simulink model could not control completely the processor use, resulting in a slight variation of sampling rate (jitter). However, this problem did not compromise the application. The exoskeleton movements are significantly slower than the sampling rate. Moreover, this problem could be solved with the use of a Real Time Operating System.

2.5 Experiment description

Fig. 3 shows the assembled prototype and auxiliary components, such as power supply, electronic drive circuit, load cell signal conditioner and the USB-6008 ADC/DAC interface.

The control tests performed on the prototype were based mostly on the works of Aguirre-Ollinger et al. (2007). However, there are important differences. Aguirre-Ollinger et al. (2007) developed a system in which the exoskeleton user should raise the leg until they reached a determined angle (visualized through a computer screen) in the shortest time possible. In this work, the experiment consisted of manipulating the prototype in order to follow a sinusoidal trajectory of the angle, which was also displayed by a screen. The force was applied to the exoskeleton as indicated in Fig. 4, tangentially to the rotation axis. The movement to raise the pendulum occurs counter-clockwise. Fig. 4 also shows the experimental setup. In the screen, it is displayed the plot generated by Simulink, where the pink line indicates the theoretical trajectory and the blue line, the actual angle of the pendulum. Detailed results are shown on Figs. 7 to 10.

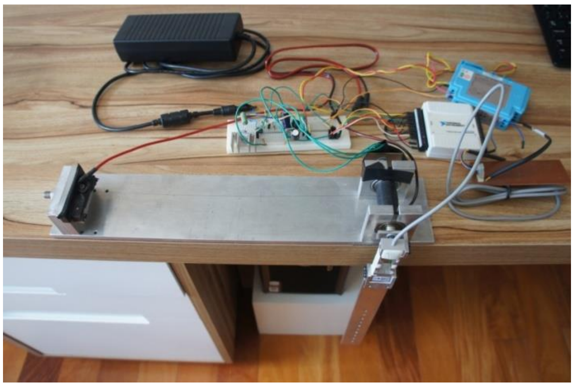

Figure 3 – Assembled prototype and auxiliary components

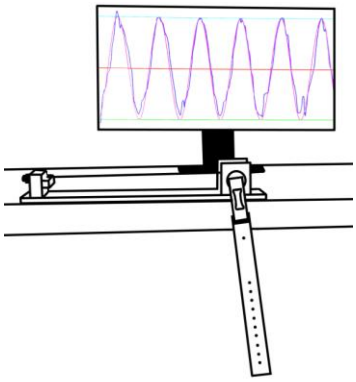

Figure 4 – Experimental setup.

3. CONTROL

The impedance control algorithm presented in this work was developed considering prior results obtained by Hogan (Hogan, 1985) and Aguirre-Ollinger et al. (Aguirre-Ollinger et al., 2007). Simulations of this algorithm were already presented by the authors (Araujo et al., 2012; Araujo, 2014).

It is important to notice that, although this controller has been implemented with SMA actuators, the proposed architecture does not depend directly on the type of actuator. Thus, it can be used in a any application that needs impedance control. The only requirement is that the actuator must have a force (or torque) control algorithm (built in or incorporated to the impedance control scheme), since the "Actuator" block (Fig. 5) receives a force or torque input and its output is the force or torque which, together with the human effort, drive the load. In addition, this impedance controller can be extended to other kinds of robotic systems, not being exclusive for exoskeletons (Araujo et al., 2012).

3.1 Formulation

In order to modify the impedance perceived by the user, the exoskeleton should exert adequate torques, depending on the angular position of the pendulum, as well as the torque applied by the user. In fact, the controller receives as input the interaction torque between the user and the exoskeleton. This signal passes through a block that contains the reciprocal of the desired impedance, which is the impedance the user would perceive while wearing the device. Then, this block outputs a position reference which feeds a PID controller that also has negative feedback of the pendulum position. The PID controller then outputs a torque reference to the actuator block, which has an embedded torque controller. The actuator output is summed to the user torque. The block diagram on Fig. 5 (Araujo et al., 2012) represents the algorithm. A Simulink program was developed to control the experimental tests, and its block diagram is depicted below on Fig. 6. The "Prototype" block is the interface between the program and the physical system. The position controller for the exoskeleton was implemented using proportional and derivative gains of 1.0 and 0.1, respectively.

The experiment aimed to confirm the results obtained previously during the simulations, as described by Araujo et al. (Araujo et al., 2012). To do so, 15 tests were made using the prototype, considering a series of parameter combinations, as described next. These parameters were selected based on limitations of the actuator (maximum frequency and range of motion) and results obtained through simulations and preliminary experimental tests.

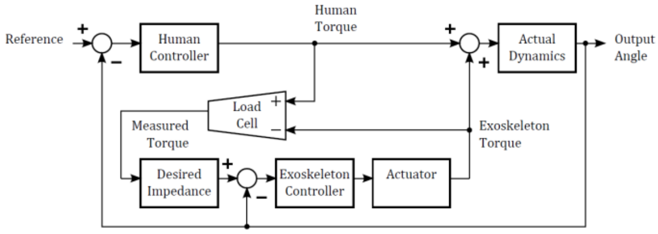

Figure 5 – Impedance control algorithm represented by a block diagram (Araujo et al., 2012).

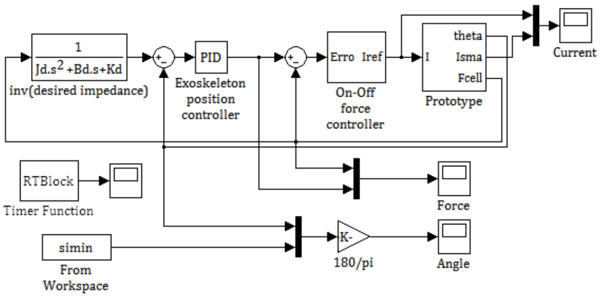

Figure 6 – Impedance control algorithm implemented on Simulink.

- Three cases of desired impedance:
  - without any reduction in the desired impedance;
  - 25% reduction;
  - 50% reduction;
- Two cases of movement range:
  - a smaller range, from 15° to 30°;
  - and a longer range, from 10° to 40°;
- Three cases of movement frequency:
  - 0.05 Hz;
  - 0.10 Hz;
  - 0.15 Hz.

Table 1 lists the configuration of each of the 15 tests.

Table 1 – Configuration of tests.

Test number	Configuration		
	Impedance	*Angle*	*Frequency*
1	Control inactive	15° - 30°	0.05 Hz
2	Zd = ½ * Zh	15° - 30°	0.05 Hz
3	Control inactive	15° - 30°	0.10 Hz
4	Zd = ½ * Zh	15° - 30°	0.10 Hz
5	Control inactive	15° - 30°	0.15 Hz
6	Zd = ½ * Zh	15° - 30°	0.15 Hz
7	Control inactive	10° - 40°	0.05 Hz
8	Zd = ½ * Zh	10° - 40°	0.05 Hz

Test number	Configuration		
	Impedance	*Angle*	*Frequency*
9	Control inactive	10° - 40°	0.10 Hz
10	Zd = ½ * Zh	10° - 40°	0.10 Hz
11	Control inactive	10° - 40°	0.15 Hz
12	Zd = ½ * Zh	10° - 40°	0.15 Hz
13	Control inactive	10° - 40°	0.05 Hz
14	Zd = ¾ * Zh	10° - 40°	0.05 Hz
15	Zd = ½ * Zh	10° - 40°	0.05 Hz

To analyze the results obtained during these experimental tests, with a focus to assess the effectiveness of the impedance controller, one of the plots shows the relationship between the impedance perceived by the human and the real impedance (human limb and exoskeleton), both estimated by the angle and torque measurements. Theoretically, the impedance perceived by the user would be equal to the desired impedance; however, in reality, there can be differences caused by imperfections in the construction of the exoskeleton, model errors and limitations of the actuators and its control.

This analysis of the impedance perceived by the user takes into account the simplification that the movement is relatively slow, i.e., the dynamics terms can be disregarded (i.e., only stiffness is considered), as it is indicated by Eq. (1).

$$\dot{\theta} \to 0 \Rightarrow J.\ddot{\theta} + B.\dot{\theta} \ll M.d.g.\sin(\theta) \qquad (1)$$

Considering this hypothesis and using the definition of impedance as torque divided by angle (Araujo, 2014), then it is defined the effective impedance, $\widehat{Z_e}$, as the estimate of the impedance perceived by the human when the exoskeleton is turned on. The effective impedance is defined by Eq. (2).

$$\widehat{Z_e}(t) = \frac{\tau(t)}{\theta(t)}\ ; controller\ active \qquad (2)$$

The real impedance of the system (human leg and exoskeleton) is calculated similarly by (3), but when the actuation is turned off (i.e., only the user exerts torque).

$$\widehat{Z_r}(t) = \frac{\tau(t)}{\theta(t)} \; ; controller\ inactive \tag{3}$$

Figure 7, next, shows the estimated impedances for tests 1 and 2, as well as the angle, to serve as reference.

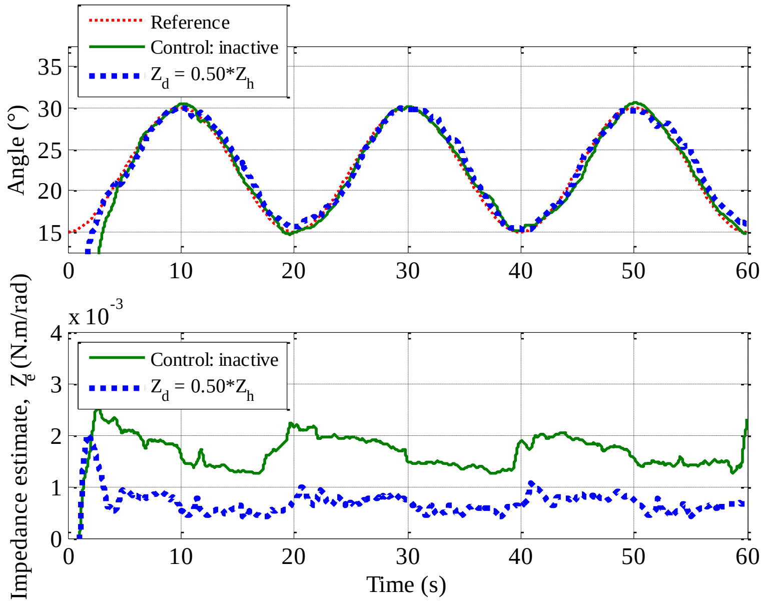

Figure 7 – Tests 1 and 2, showing angle and estimated impedance.

These results show that, with the control active, there has been a significant reduction in the impedance perceived by the human. Since in both tests the objective was to track the reference angle trajectory, and assuming that the error is low compared to the movement in this case (almost always less than 2°, absolute value), it is defined the impedance ratio, R_Z, then calculated by the Eq. (4).

$$R_Z(t) = \frac{\widehat{Z_e}(t)}{\widehat{Z_r}(t)} \tag{4}$$

Figure 8 shows the complete results of tests 1 and 2. In these cases, the angle ranges from 15° to 30° and the frequency of the movement is 0.05 Hz. In test 2, it is possible to notice an important reduction of the torque exerted by the human, when compared to test 1 (in which only the user applied torque to move the limb and exoskeleton). Moreover, the controller kept the effective impedance close to the desired value of 50% during the whole movement of the exoskeleton.

Next, Fig. 9 presents the results of tests 3 and 4. In these tests, the movement frequency was increased to 0.10 Hz. It can be seen that the exoskeleton performance is already degraded in the return movement (from 30° to 15°), despite this is observed as a further reduction in perceived impedance.

Increasing the range of motion, Fig. 10 displays the data obtained from tests 7 and 8, with angles from 10° to 40° and frequency of 0.05 Hz. In this case, the desired impedance was achieved from 10° to 30°, but above 30° the exoskeleton loses efficiency.

The results of tests 9 and 10 are presented in Fig. 11. In these instances, the movement frequency raised to 0.10 Hz. It can be seen that both the increase in movement range (when compared to tests 2 and 4) and frequency make it difficult to control the desired impedance. For the sake of space, the results of tests at 0.15 Hz are not presented here. However, the performance at this frequency is very limited due to the poor actuator frequency response. The complete results can be found on (Araujo, 2014). With 0.15 Hz movement, the impedance ratio plot looks similar to the correspondent result in test 10.

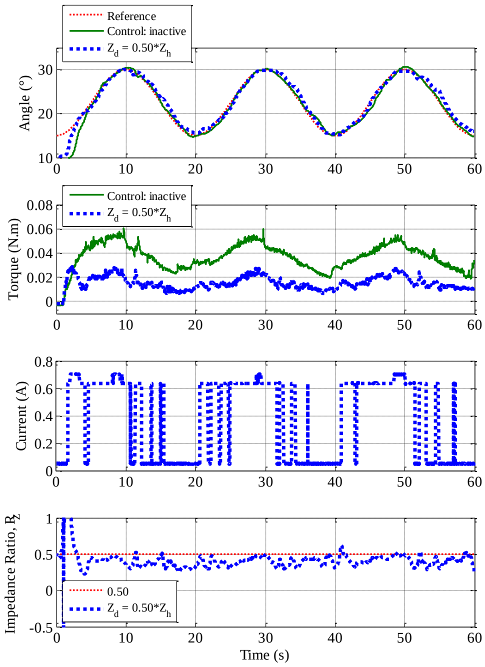

Figure 8 – Tests 1 and 2; 15° to 30°, 0.05 Hz

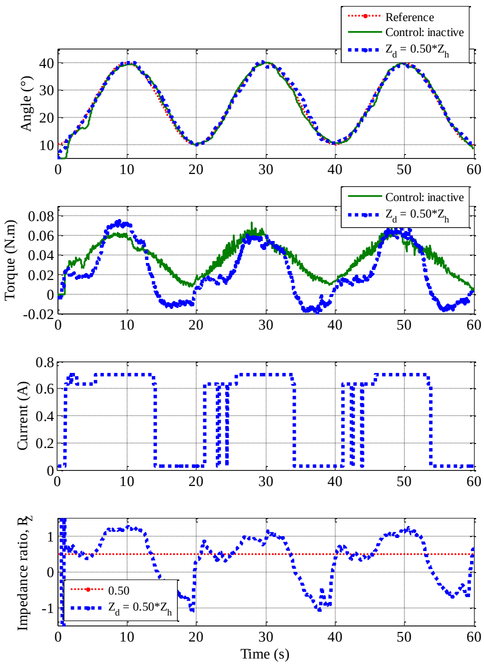

Figure 10 – Tests 7 and 8; 10° to 40°, 0.05 Hz

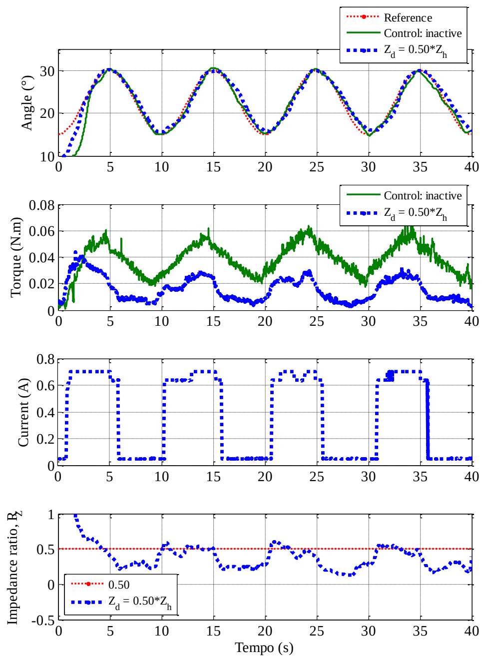

Figure 9 – Tests 3 and 4; 15° to 30°, 0.10 Hz

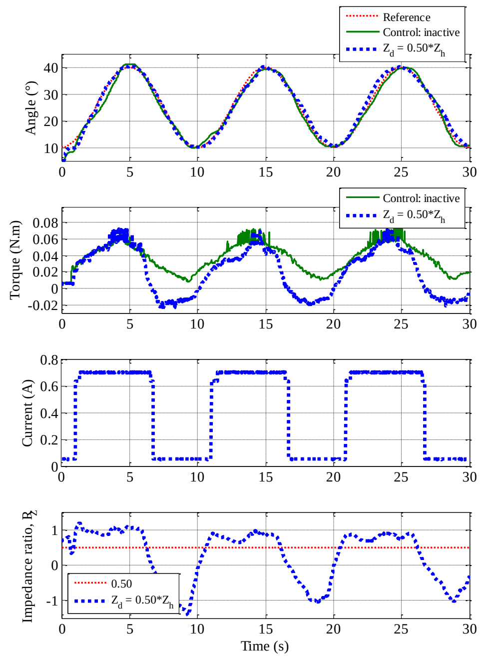

Figure 11 – Tests 9 and 10; 10° to 40°, 0.10 Hz

In the last series of tests to be analyzed, it was evaluated the influence of the desired impedance parameter, by selecting two values: reduction of 25% and 50% in relation to the real impedance. The results are presented below in Fig. 12. In these 3 tests, the angle range from 10° to 40° and the frequency is 0.05 Hz.

This time, only one cycle is analyzed. In test 14, where the desired reduction in impedance was 25%, the controller maintained the effective impedance close to the desired value approximately between 20s (15°) and 26s (35°); between 26s and 32.5s, the exoskeleton loses efficiency; after 32.5s, the return movement is restrained by the actuator, demanding the user to apply additional torque to lower the pendulum. In test 15, with desired impedance equal to 50% of the real one, the controller functions similarly to the previous case. Approximately between instants 20s (15°) and 28s (35°), the effective impedance is kept within the range of the desired values; between instants 28s and 31s, the effective impedance raises, and then falls back again when the pendulum starts to return to 10° position. Once more, the return movement is restrained by the actuator.

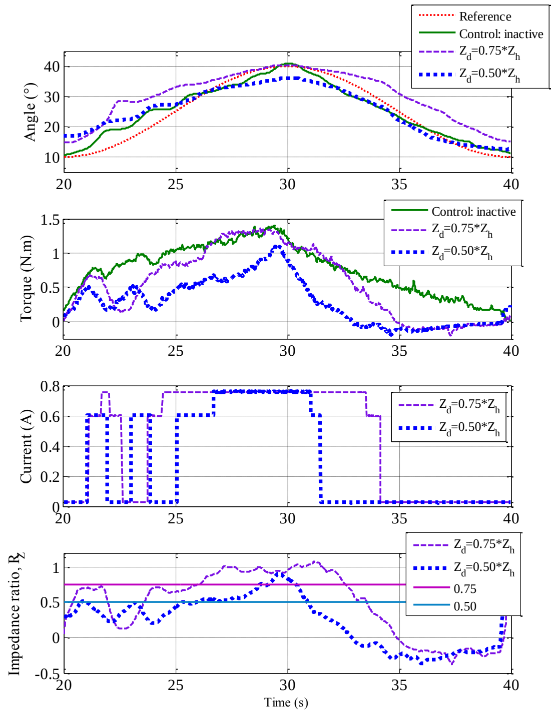

Figure 12 – Tests 13, 14 and 15; 10° to 40°, 0.05 Hz, variable desired impedance: 100%, 75% and 50% of the real value.

4. DISCUSSION

Considering the results presented, the control algorithm has been proven to work in the prototype, confirming the simulations (Araujo et al., 2012; Araujo, 2014). SMA actuators have advantages when compared to conventional actuators, such as high power-to-weight ratio and flexibility, which are interesting when building exoskeletons. However, this kind of actuation still have a series of technical and technological burdens that have yet to be overcome before SMA actuators are to be seen on exoskeletons for humans. The most prominent difficulties related to the actuator could be summarized in three topics.

- Very small bandwidth: both in the simulations (Araujo et al., 2012; Araujo, 2014) and experimental tests, the maximum movement frequency that resulted in acceptable performance was in the order of 0.10 Hz. Above that, the cooling of the wire is not fast enough to allow the pendulum to return without additional effort from the user. In order to be used with humans, the exoskeleton should have at least a bandwidth in the order of 1 Hz (Nilsson, Thorstendsson, 1987). This limitation also made it impossible to evaluate the dynamic components of impedance, since the actuator is not effective for higher frequencies of movement.
- Limited range of motion: the SMA wire features a length variation of about 4% of maximum length. With the view to increase the movement it is necessary to use longer wires (which require greater electrical power to be driven, due to the higher ohmic resistance) or apply amplification devices such as gears or pulleys (which inevitably decreases the force proportionally to the movement increase).
- Dependence on temperature: the actuator is based on the change of the wire temperature; therefore it depends on the electrical driver current capacity and also on the environmental conditions.

4.1 Further development

With regards to the actuator, it is clear that the cooling must be improved. Several ideas could be employed, for example: thermoelectric elements (Romano, Tannuri, 2009b); water (Mascaro, Asada, 2003); or even mechanical heat sinks (Russel, Gorbet, 1995). Another aspect that could improve the frequency response would be to use an antagonistic setup, which could be active (with a reciprocal SMA wire (Romano, Tannuri, 2009a)), or even passive, by the use of a spring. As for the impedance control, the fact that experimental tests confirmed the simulations indicates it feasibility to be implemented in an actual exoskeleton for humans.

5. CONCLUSION

The experimental apparatus necessary to evaluate the feasibility of the proposed impedance control architecture was designed and constructed, allowing the conduction of tests, which confirmed the simulations' results. Despite of the complications enumerated, it is not possible to discard the possibility of using SMA actuators in exoskeletons for humans. The concepts that were elaborated during this work were first simulated and then tested and validated in the prototype. Advancements in SMA technology and improvements to the control architecture could make it possible to build a human scale exoskeleton with this kind of actuator.

6. ACKNOWLEDGMENTS

The second author thanks the CNPq (process 308645/2013-8) for the research grant.

7. REFERENCES

Activelink Co., Ltd., 2014. "POWERLOADER light 'PLL'". <http://psuf.panasonic.co.jp/alc/en/technologies/020-pll-power-loader-light.html>.

Aguirre-Ollinger, g., Colgate, J. E., Peshkin, M. A., Goswami, A., 2007. "A 1-DOF assistive exoskeleton with virtual negative damping: effects on the kinematic response of the lower limbs". *IEEE/RSJ International conference on intelligent robots and systems, pp. 1938-1944*.

Aral, F., Azuma, D., Narumi, K., Yamanishi, Y., Lin, Y.C., 2007. "Design and fabrication of a shape memory alloy actuated exoskeletal microarm". *International Symposium on Micro-NanoMechatronics and Human Science, pp. 339-343*.

Araujo, A.A.M., 2014. "Desenvolvimento de controle de impedância aplicado a exoesqueleto biomecatrônico atuado por liga de memória de forma". University of São Paulo.

Araujo, A.A.M.; Tannuri, E.A.; Forner-Cordero, A., 2012. "Simulation of model-based impedance control applied to a biomechatronic exoskeleton with shape memory alloy actuators". *2012 4th IEEE RAS & EMBS International Conference on Biomedical Robotics and Biomechatronics (BioRob), pp.1567-1572*.

Crowell III, H. P., Boynton, A. C., Mungiole, M., 2002. "Exoskeleton power and torque requirements based on human biomechanics". *Army Research Laboratory, Technical Report ARL-TR-2764*.

Cyberdyne, 2012. "Robot Suit HAL®". <http://www.cyberdyne.jp/english/robotsuithal/>

Daga, L., 2012. "RT Blockset". <http://leonardodaga.insyde.it/Simulink/RTBlockset.htm>

De Laurentis, K.J.; Fisch, A.; Nikitczuk, J.; Mavroidis, C., 2002. "Optimal design of shape memory alloy wire bundle actuators". *IEEE International Conference on Robotics and Automation, vol.3*, pp.2363-2368.

Dollar, A. M., Herr, H., 2008. "Lower Extremity Exoskeletons and Active Orthoses: Challenges and State-of-the-Art". *IEEE Transactions on Robotics, vol. 24, no. 1, pp. 144-158*.

Ekso Bionics, 2014. "Ekso Bionics – Exoskeleton, wearable robot for people with paralysis from SCI or stroke". <http://eksobionics.com/ekso>

Hogan, N., 1985. "Impedance control: an approach to manipulation". *Journal of Dynamic Systems, Measurement and Control, vol. 107, pp. 1-24*.

Kim, H. K., Carmena, J. M., Biggs, S. J., Hanson, T. L., Nicolelis, M. A. L., Srinivasan, M. A., 2007. "The Muscle Activation Method: An Approach to Impedance Control of Brain-Machine Interfaces Through a Musculoskeletal Model of the Arm". *IEEE Transactions on Biomedical Engineering, vol. 20, no. 8, pp. 1520-1529*.

Lu, A., Grant, D., Hayward, V., 1997. "Design and Comparison of High Strain Shape Memory Alloy Actuators". *IEEE International Conference on Robotics and Automation, vol. 1, pp. 260-265*.

Mascaro, S. A., Asada, H. H., 2003. "Wet shape memory alloy actuators for active vasculated robotic flesh". *ICRA '03 IEEE International Conference on Robotics and Automation, v. 1, pp. 282-287*.

Miranda, A.B.W.; Yasutomi, A.Y.; Souit, C.; Forner-Cordero, A., 2012. "Bioinspired mechanical design of an upper limb exoskeleton for rehabilitation and motor control assessment". *2012 4th IEEE RAS & EMBS International Conference on Biomedical Robotics and Biomechatronics (BioRob) , pp.1776-1781*.

Nilsson, J., Thorstensson, A., 1987. "Adaptability in frequency and amplitude of leg movements during human locomotion at different speeds". *Acta Physiologica Scandinavica, v. 129:, pp. 107–114*.

Raparelli, T., Zobel, P. B., Durante, F., 2002. "A Robot Actuated BR Shape Memory Alloy Wires". *IEEE International Symposium on Industrial Electronics, vol. 2, pp. 420-423*.

Romano, R., Tannuri, E. A., 2009a. "Comparison between single-wire and antagonistic shape memory alloy actuators". *XIII International Symposium on Dynamic Problems of Mechanics (DINAME 2009)*.

Romano, R., Tannuri, E. A., 2009b. "Modeling, control and experimental validation of a novel actuator based on shape memory alloys". *Mechatronics (Oxford), v. 19, pp. 1169-1177*.

Russel, R. A., Gorbet, R. B., 1995. "Improving the response of SMA actuators". *Proceedings of the 1995 IEEE International Conference on Robotics and Automation, v. 3, pp. 2299-2304*.

8. RESPONSIBILITY NOTICE